arXiv:1811.00825v1 [math.NA] 2 Nov 2018

PRIMAL DUAL MIXED FINITE ELEMENT METHODS FOR INDEFINITE ADVECTION–DIFFUSION EQUATIONS *

ERIK BURMAN † AND CUIYU HE ‡

Abstract. We consider primal-dual mixed finite element methods for the advection–diffusion equation. For the primal variable we use standard continuous finite element space and for the flux we use the Raviart-Thomas space. We prove optimal a priori error estimates in the energy- and the L^2-norms for the primal variable in the low Peclet regime. In the high Peclet regime we also prove optimal error estimates for the primal variable in the $H(div)$ norm for smooth solutions. Numerically we observe that the method eliminates the spurious oscillations close to interior layers that pollute the solution of the standard Galerkin method when the local Peclet number is high. This method, however, does produce spurious solutions when outflow boundary layer presents. In the last section we propose two simple strategies to remove such numerical artefacts caused by the outflow boundary layer and validate them numerically.

Key words. Advection–Diffusion, Primal Dual Method, Mixed Finite Element Method

AMS subject classifications. 65N30

1. Introduction.

Advection–diffusion problems have been extensively studied in the last decades for its wide applications in the area of weather-forecasting, oceanography, gas dynamics, contaminant transportation in porous media, to name a few. Many numerical methods for advection–diffusion equations have been explored in the literature. The two main concerns when designing a numerical method for advection–diffusion problems are robustness in the advection dominated limit and satisfaction of local conservation. The standard Galerkin method, using globally continuous approximation, is known to fail on both points and therefore much effort has been devoted to the design of alternative formulations. Typically to make the method stable in the limit of dominating advection some stabilizing operator is introduced to provide sufficient control of fine scale fluctuations. The most well known stabilized method is the Streamline upwind Petrov Galerkin method (SUPG) introduced by Hughes and co-workers [6] and first analyzed by Johnson and co-workers [32]. In order to avoid disadvantages associated to the Petrov-Galerkin character, for instance related to time discretization, the discontinuous Galerkin method was introduced, first in the context of hyperbolic transport [33, 22]. In this case the stabilizing mechanism is due to the upwind flux, which controls the solution jump over element faces and adds a dissipation proportional to this jump. In the context of finite element methods using H^1-conforming approximation several stabilized methods using symmetric stabilization have been proposed, for instance the subgrid viscosity method by Guermond [30], the orthogonal subscale method by Codina [23], the continuous interior penalty method (CIP), introduced by Douglas and Dupont [27] and analyzed by Burman and Hansbo [13]. It is well known that for both cases of discontinuous and continuous approximation spaces a local conservative numerical flux can be defined. In the continuous case, however, it must be reconstructed using post processing [31, 16].

In this work, to ensure local conservation of the computed flux we design a method in the mixed setting: we approximate the primal variable in the standard conform-

* This work was funded by the EPSRC grant EP/P01576X/1.

†Department of Mathematics, University College London, Gower Street, London, UK–WC1E 6BT, United Kingdom (e.burman@ucl.ac.uk)

‡Department of Mathematics, University College London, Gower Street, London, UK–WC1E 6BT, United Kingdom (c.he@ucl.ac.uk)

ing finite element space and the flux in the Raviart-Thomas space. The numerical scheme is based on a constrained minimization problem in which the difference between the flux variable and the flux evaluated using the primal variable is minimized under the constraint of the conservation law. The method is very robust and was initially introduced for the approximation of ill-posed problems, such as the elliptic Cauchy problem, see [14]. Herein we consider well-posed, but possibly indefinite advection–diffusion equations. However, the results extend to ill-posed advection–diffusion equations using the ideas of [14] and [15].

Indefinite, or noncoercive, elliptic problems with Neumann boundary conditions were considered first in [17] and more recently in [18, 34, 8] using finite volume and finite element methods. The method proposed herein is a mixed variant of the primal-dual stabilized finite element method introduced in [8, 11] for the respective indefinite elliptic and hyperbolic problems, drawing on earlier ideas on H^{-1}-least square methods from [4]. Contrary to those work we herein consider a formulation where the approximation spaces are chosen so that it is inf-sup stable. Hence no stabilizing terms are required. Primal dual methods without stabilization were proposed for the advection–diffusion problem in [19] and for second order PDE in [3, 2], inspired by previous work on Petrov-Galerkin methods [26, 25]. Similar ideas have recently been exploited successfully in the context of weak Galerkin methods for elliptic problems on non-divergence form [40], Fokker-Planck equations [39], and the ill-posed elliptic Cauchy problem in [41]. In [35] a method was introduced which is reminiscent of the lowest order version of the method we propose herein. The case of high Peclet number was, however, not considered in [35], so our analysis is likely to be useful for the understanding of the method in [35] in this regime.

1.1. Main results. For the error analysis, in the low Peclet regime, we prove optimal convergence orders for the L^2- and H^1- norms for the primal variable for all polynomial orders. For the analysis we do not use coercivity, but only the stability of the solution, showing the interest of the method for indefinite (or T-coercive [20]) problems. In the high Peclet regime we assume that the data of the adjoint operator satisfy a certain positivity criterion, which is different to the classical one for coercivity. We then prove an error estimate in negative norm and optimal order convergence of the error in the streamline derivative of the primal variable measured in the L^2- norm, for smooth solutions.

Numerical results for both the diffusion- and advection-dominated problems are presented. Optimal convergence is verified on smooth problems and on a problem with reduced regularity due to a corner singularity. We note that for problems with an internal layer only mild and localized oscillations are observed (see Figure 2). However, for problems with under-resolved outflow boundary layers the effect of the layer causes global pollution of the solution (see Figure 1). In section 6 we propose two simple strategies to improve the method in this case. More specifically, one method imposes the boundary condition weakly and the second approach introduces a weighting of the stabilizer such that the oscillation is more "costly" closer to the inflow boundary. This latter variant introduces a notion of upwind direction.

This paper is organized as follows. In section 2, the model problem is presented. The numerical scheme is proposed and its stability and continuity is analyzed in section 3. In section 4, we prove the error estimation results for both problems with either low or high Peclet numbers. Numerical results are presented in section 5. In section 6 we propose two strategies to improve accuracy in the presence of under-resolved outflow boundary layers. Numerical results are also presented to test their

effectiveness.

2. The Model Problem. Let $\Omega \in \mathbb{R}^d$, $d \in \{2,3\}$, be a polygonal/polyhedral domain, with boundary $\partial\Omega$ and outward pointing unit normal $\boldsymbol{n}$. We consider the following advection–diffusion equation,

$$\nabla \cdot (\boldsymbol{\beta} u - A\nabla u) + \mu u = f \tag{2.1}$$

with the boundary conditions

$$\begin{aligned} u &= g \text{ on } \Gamma_D, \quad \text{and} \\ (A\nabla u - \boldsymbol{\beta} u)\cdot \boldsymbol{n} &= \psi \text{ on } \Gamma_N. \end{aligned} \tag{2.2}$$

where Γ_D, $\Gamma_N \subset \partial\Omega$, $\Gamma_D \cap \Gamma_N = \emptyset$ and $\bar{\Gamma}_D \cup \bar{\Gamma}_N = \partial\Omega$. For simplicity, we assume that $\Gamma_D \neq \emptyset$. The problem data is given by $f \in L^2(\Omega)$, $g \in H^{\frac{1}{2}}(\Gamma_D)$, $\psi \in H^{-\frac{1}{2}}(\Gamma_N)$, $A \in \mathbb{R}^{d\times d}$, $\mu \in \mathbb{R}$ and $\boldsymbol{\beta} \in [L^\infty(\Omega)]^d$, with $\boldsymbol{\beta}_\infty := \|\boldsymbol{\beta}\|_{L^\infty(\Omega)}$. For the analysis in the advection dominated case we will strengthen the assumptions on the parameters. Furthermore, we assume that the matrix A is symmetric positive definite. With the smallest eigenvalue $\lambda_{min,A} > 0$ and the largest eigenvalue $\lambda_{\max,A}$ we assume that $\lambda_{\max,A}/\lambda_{min,A}$ is bounded by a moderate constant. The below analysis holds also in the case of variable A and μ, that are piecewise differentiable on polyhedral subdomains, provided ajustements are made for loss of regularity in the exact solution.

Let

$$V_{g,D} = \{v \in H^1(\Omega) : v = g \text{ on } \Gamma_D\} \quad \text{and} \quad V_{0,D} = \{v \in H^1(\Omega) : v = 0 \text{ on } \Gamma_D\}. \tag{2.3}$$

Consider the weak form: find $u \in V_{g,D}$ such that

$$a(u,v) = l(v), \quad \forall\, v \in V_{0,D}, \tag{2.4}$$

with

$$a(u,v) := (\mu u, v)_\Omega + (A\nabla u - \boldsymbol{\beta} u, \nabla v)_\Omega,$$

and

$$l(v) := (f,v)_\Omega + \langle \psi, v\rangle_{\Gamma_N},$$

where $(\cdot,\cdot)_w$ denotes the L^2 inner product on w. When w coincides with the domain Ω the subscript is omitted below. We will only assume that the problem satisfies the Babuska-Lax-Milgram theorem [1], which, in the case of homogenous Dirichlet condition, implies the existence and uniqueness and the following stability estimate

$$\|u\|_V \leq \alpha^{-1}\|l\|_{V'},$$

where $\|\cdot\|_V$ is the H^1-norm, α is the constant of the inf-sup condition and the dual norm is defined by

$$\|l\|_{V'} := \sup_{\substack{v\in V \\ \|v\|_V = 1}} l(v).$$

Observe that in the case of heterogenous Dirichlet condition we may write $u = u_0 + u_g$ where $u_0 \in V_{0,D}$ is unknwon and $u_g \in V_{g,D}$ is a chosen lifting of the boundary data such that $\|u_g\|_V \leq \|g\|_{H^{\frac{1}{2}}(\Gamma_D)}$. In that case the stability may be written as

$$\|u_0\|_V \leq \alpha^{-1}\|l_g\|_{V'}, \tag{2.5}$$

where $l_g(v) = l(v) - a(u_g, v)$.

3. The Mixed Finite Element Framework.

3.1. Some preliminary results. Let $\{\mathcal{T}\}_h$ be a family of conforming, quasi uniform triangulations of Ω consisting of shape regular simplices $\mathcal{T} = \{K\}$. The diameter of a simplex K will be denoted by h_K and the family index h is the mesh parameter defined as the largest diameter of all elements, i.e, $h = \max_{K\in\mathcal{T}}\{h_K\}$. We denote by $\mathcal{F}$ the set of all faces in $\mathcal{T}$, by $\mathcal{F}_I$ the set of all interior faces in $\mathcal{T}$ and by $\mathcal{F}_D$ and $\mathcal{F}_N$ the sets of faces on the respective Γ_D and Γ_N. For each $F \in \mathcal{F}$ denote by $\boldsymbol{n}_F$ a unit vector normal to F and $\boldsymbol{n}_F$ is fixed to be outer normal to $\partial\Omega$ when F is a boundary face.

Frequently, we will use the notation $a \lesssim b$ meaning $a \leq Cb$ where C is a non-essential constant, independent of h. Significant properties of the hidden constant will be highlighted.

We denote the standard H^1-conforming finite element space of order k by

$$V_h^k := \{v_h \in H^1(\Omega) : v|_K \in \mathbb{P}_k(K), \quad \forall\, K \in \mathcal{T}\}$$

where $\mathbb{P}_k(K)$ denotes the set of polynomials of degree less than or equal to k in the simplex K. Let $i_h : C^0(\bar{\Omega}) \mapsto V_h^k$ be the nodal interpolation. The following approximation estimate is satisfied by i_h, see e.g., [28]. For $v \in H^{k+1}(\Omega)$ there holds

$$\|v - i_h v\| + h\|\nabla(v - i_h v)\| \lesssim h^{k+1}|v|_{H^{k+1}(\Omega)}, \quad k \geq 1. \tag{3.1}$$

For the primal variable we introduce the following spaces

$$V_{g,D}^k := \{v_h \in V_h^k \,:\, v_h = g_h \text{ on } \Gamma_D\} \quad \text{and} \quad V_{0,D}^k := \{v_h \in V_h^k \,:\, v_h = 0 \text{ on } \Gamma_D\},$$

where g_h is the nodal interpolation of g (or if g has insufficient smoothness, some other optimal approximation of g) on the trace of Γ_D so that g_h is piecewise polynomial of order k with respect to $\mathcal{F}_D$.

For the flux variable we use the Raviart-Thomas space

$$RT^l := \{\boldsymbol{q}_h \in H_{div}(\Omega) \,:\, \boldsymbol{q}_h|_K \in \mathbb{P}_l(K)^d \oplus \boldsymbol{x}(\mathbb{P}_l(K) \setminus \mathbb{P}_{l-1}(K)),\ \forall\, K \in \mathcal{T}\},$$

with $\boldsymbol{x} \in \mathbb{R}^d$ being the spatial variable, $l \geq 0$ and $\mathbb{P}_{-1}(K) \equiv \emptyset$. We recall the Raviart-Thomas interpolant $\boldsymbol{R}_h : H^1(div, \Omega) \mapsto RT^l$, where

$$H^m(div, \Omega) := \left\{\boldsymbol{w} \in [H^m(\Omega)]^d \,:\, \nabla \cdot \boldsymbol{w} \in H^m(\Omega)\right\},$$

and its approximation properties [28]. For $\boldsymbol{q} \in H^m(div, \Omega)$, $m \geq 1$ and $\boldsymbol{R}_h\boldsymbol{q} \in RT^l$, there holds

$$\|\boldsymbol{q} - \boldsymbol{R}_h\boldsymbol{q}\|_\Omega + \|\nabla \cdot (\boldsymbol{q} - \boldsymbol{R}_h\boldsymbol{q})\|_\Omega \lesssim h^r(|\nabla \cdot \boldsymbol{q}|_{H^r(\Omega)} + |\boldsymbol{q}|_{H^r(\Omega)}) \tag{3.2}$$

where $r = \min(m, l + 1)$.

We also introduce the L^2-projection on the face F of some simplex $K \in \mathcal{T}$,

$$\pi_{F,l} : L^2(F) \mapsto \mathbb{P}_l(F)$$

such that for any $\phi \in L^2(F)$

$$\langle \phi - \pi_{F,l}(\phi), p_h \rangle_F = 0, \quad \forall\, p_h \in \mathbb{P}_l(F).$$

Then by assuming that the Neumann data ψ is in $L^2(\Gamma_N)$ we define the discretized Neumann boundary data by its L^2-projection such that for each $F \in \mathcal{F}_N$ we have $\psi_h|_F := \pi_{F,l}(\psi)$. With the satisfaction of the Neumann condition built in, we define

$$RT^l_{\psi,N} = \{\boldsymbol{q}_h \in RT^l : \boldsymbol{q}_h \cdot \boldsymbol{n} = -\psi_h \text{ on } \Gamma_N\}$$

and

$$RT^l_{0,N} = \{\boldsymbol{q}_h \in RT^l : \boldsymbol{q}_h \cdot \boldsymbol{n} = 0 \text{ on } \Gamma_N\}.$$

For the Lagrange multiplier variable, we introduce the space of functions in $L^2(\Omega)$ that are piecewise polynomial of order m in each element by

$$X^m_h := \{x_h \in L^2(\Omega) : x_h|_K \in \mathbb{P}_m(K), \quad \forall\, K \in \mathcal{T}\}.$$

We define the L^2-projection $\pi_{X,m} : L^2(\Omega) \mapsto X^m_h$ such that

$$(y - \pi_{X,m}(y), x_h) = 0, \quad \forall\, x_h \in X^m_h.$$

For functions in X^m_h we define the broken norms,

$$\|x\|_h := \left(\sum_{K\in\mathcal{T}} \|x\|^2_K\right)^{\frac{1}{2}} \text{ and } \|x\|_{1,h} := \left(\|\nabla x\|^2_h + \|h^{-\frac{1}{2}}[\![x]\!]\|^2_{\mathcal{F}_I\cup\mathcal{F}_D}\right)^{\frac{1}{2}} \tag{3.3}$$

where $\|h^{-1/2}x\|^2_{\mathcal{F}_I\cup\mathcal{F}_D} := \sum_{F\in\mathcal{F}_I\cup\mathcal{F}_D} h_F^{-1}\|x\|^2_F$ and

$$[\![x]\!]|_F(z) := \begin{cases} \lim\limits_{\epsilon\to 0^+} (x(z - \epsilon\boldsymbol{n}_F) - x(z + \epsilon\boldsymbol{n}_F)) & \text{for } F \in \mathcal{F}_I, \\ x(z) & \text{for } F \in \mathcal{F}_D \cup \mathcal{F}_N. \end{cases}$$

Also recall the discrete Poincaré inequality [5],

$$\|x\| \lesssim \|x\|_{1,h}, \quad \forall\, x \in X^m_h, \tag{3.4}$$

which guarantees that $\|\cdot\|_{1,h}$ is a norm.

Given a function $x_h \in X^m_h$ we define a reconstruction, $\boldsymbol{\eta}_h(x_h) \in RT^l_{0,N}$, of the gradient of x_h such that for all $F \in \mathcal{F}_I \cup \mathcal{F}_D$

$$\langle \boldsymbol{\eta}_h(x_h)\cdot\boldsymbol{n}_F, p_h\rangle_F = \left\langle h_F^{-1}[\![x_h]\!], p_h\right\rangle_F, \quad \forall\, p_h \in \mathbb{P}_l(F), \tag{3.5}$$

where h_F is the diameter of F, and if $l \geq 1$, for all $K \in \mathcal{T}$,

$$(\boldsymbol{\eta}_h(x_h), \boldsymbol{q}_h)_K = -(\nabla x_h, \boldsymbol{q}_h)_K, \quad \forall\, \boldsymbol{q}_h \in [\mathbb{P}_{l-1}(K)]^d. \tag{3.6}$$

We prove the stability of $\boldsymbol{\eta}_h$ with respect to the data in the following proposition.

PROPOSITION 3.1. *There exists an unique $\boldsymbol{\eta}_h \in RT^l_{0,N}$ such that (3.5)–(3.6) hold. Moreover $\boldsymbol{\eta}_h$ satisfies the following stability estimate*

$$\|\boldsymbol{\eta}_h\| \leq C_{ds}\left(\|\pi_{X,l-1}\nabla x_h\|^2_h + \|h^{-\frac{1}{2}}\pi_{F,l}([\![x_h]\!])\|^2_{\mathcal{F}_I\cup\mathcal{F}_D}\right)^{\frac{1}{2}}, \tag{3.7}$$

here $C_{ds} > 0$ is a constant depending only on the element shape regularity.

Proof. We refer to [14] for the proof. ∎

We will also frequently use the following inverse and trace inequalities,

$$\|\nabla v\|_K \lesssim h^{-1}\|v\|_K, \quad \forall\, v \in \mathbb{P}_k(K) \tag{3.8}$$

and

$$\|v\|_{\partial K} \lesssim h^{-\frac{1}{2}}\|v\|_K + h^{\frac{1}{2}}\|\nabla v\|_K, \quad \forall\, v \in H^1(K). \tag{3.9}$$

For a proof of (3.8) we refer to Ciarlet [21], and for (3.9) see, e.g., Monk and Süli [38].

3.2. The finite element method. The problem takes the form of finding the critical point of a Lagrangian $\mathcal{L} : (v_h, \boldsymbol{q}_h, x_h) \in V^k_{g,D} \times RT^l_{\psi,N} \times X^m_h \mapsto \mathbb{R}$ defined by

$$\mathcal{L}[v_h, \boldsymbol{q}_h, x_h] := \frac{1}{2} s[(v_h, \boldsymbol{q}_h), (v_h, \boldsymbol{q}_h)] + b(\boldsymbol{q}_h, v_h, x_h) - (f, x_h). \tag{3.10}$$

Here $x_h \in X^m_h$ is the Lagrange multiplier, $s(\cdot,\cdot)$ denotes the primal stabilizer

$$s[(v, \boldsymbol{q}), (v, \boldsymbol{q})] := \frac{1}{2}\|\boldsymbol{\beta} v - A\nabla v - \boldsymbol{q}\|^2, \tag{3.11}$$

and $b(\cdot,\cdot)$ is the bilinear form defining the partial differential equation, in our case the conservation law,

$$b(\boldsymbol{q}_h, v_h, x_h) := (\nabla \cdot \boldsymbol{q}_h + \mu v_h, x_h).$$

By computing the Euler-Lagrange equations of (3.10) we obtain the following linear system: find $(u_h, \boldsymbol{p}_h, z_h) \in V^k_{g,D} \times RT^l_{\psi,N} \times X^m_h$ such that

$$s[(u_h, \boldsymbol{p}_h), (v_h, \boldsymbol{q}_h)] + b(\boldsymbol{q}_h, v_h, z_h) = 0, \tag{3.12}$$

$$b(\boldsymbol{p}_h, u_h, x_h) - (f, x_h) = 0, \tag{3.13}$$

for all $(v_h, \boldsymbol{q}_h, x_h) \in V^k_{0,D} \times RT^l_{0,N} \times X^m_h$. The system (3.12)–(3.13) is of the same form as that proposed in [9, 12] but without the adjoint stabilization. Therefore, to ensure that the system is well-posed the spaces $V^k_h \times RT^l \times X^m_h$ must be carefully balanced. Herein we will restrict the discussion to the equal order case $k = l = m$ that is stable without further stabilization. The arguments can be extended to other choices of spaces provided suitable extra stabilizing terms are added (see [14] for details).

Observe that the stabilizer in equation (3.11) connects the flux and the primal variables and, more precisely, brings $\boldsymbol{p}_h$ and $\boldsymbol{\beta} u_h - A\nabla u_h$ to be close. In the low Peclet regime this introduces an effect similar to the penalty on the gradient of the primal variable used in [8]. In the high Peclet regime, on the other hand, the stability of the streamline derivative is obtained by the strong control of the conservation law residual obtained through equation (3.13).

Remark 3.1. The constrained-minimization problem introduces an auxiliary variable, i.e., the Lagrange multiplier, which for stability reasons must be chosen as the discontinuous counterpart of the discretization space for the primal variable (unless stabilization is applied, see [14]). This results in a system with a substantially larger number of degrees of freedom than the standard Galerkin and the classical mixed method. Nevertheless, it is possible to reduce the system used in the iterative solver to a positive definite symmetric matrix where the Lagrange multiplier has been eliminated. This is achieved by iterating on a least square formulation and the solution of which is not locally mass conservative but has similar approximation properties. The number of degrees of freedom of the reduced system is comparable to that of the mixed method using the Raviart-Thomas element. For a detailed discussion of this approach we refer to [14].

3.3. Approximation, continuity and inf-sup condition. For the analysis we introduce the energy norms on $H^1(\Omega) \times H(div, \Omega)$,

$$|||(v, \boldsymbol{q})|||_{-1} := \left(s[(v, \boldsymbol{q}), (v, \boldsymbol{q})] + \|h(\nabla \cdot \boldsymbol{q} + \mu v)\|^2\right)^{\frac{1}{2}}, \tag{3.14}$$

$$|||(v, \boldsymbol{q})|||_\sharp := |||(v, \boldsymbol{q})|||_{-1} + \|\mu v\| + \|h^{\frac{1}{2}} \boldsymbol{q}\|_{\mathcal{F}} + \|\boldsymbol{q}\|_\Omega. \tag{3.15}$$

To quantify the dpendence of the physical parameters in the bounds below we introduce the factor $c_u := \boldsymbol{\beta}_\infty h + \|A\|_\infty + |\mu| h$.

LEMMA 3.1 (Approximation). *For any $v \in H^{k+1}(\Omega)$ and $\boldsymbol{q} \in H^{l+1}(\Omega)^d$ the following approximation properties hold:*

$$|||(v - i_h v, \boldsymbol{q} - R_h \boldsymbol{q})|||_{-1} \leq |||(v - i_h v, \boldsymbol{q} - R_h \boldsymbol{q})|||_\sharp \lesssim c_u h^k |v|_{H^{k+1}(\Omega)} + h^{l+1} |\boldsymbol{q}|_{H^{l+1}(\Omega)}. \tag{3.16}$$

Proof. Applying the triangle inequality and the approximation properties (3.1) and (3.2) gives

$$|||(v - i_h v, \boldsymbol{q} - R_h \boldsymbol{q})|||_{-1} \lesssim \left(\boldsymbol{\beta}_\infty h + \|A\|_\infty + |\mu| h^2\right) h^k |v|_{H^{k+1}(\Omega)} + h^{l+1} |\boldsymbol{q}|_{H^{l+1}(\Omega)}. \tag{3.17}$$

To estimate the remaining terms note that the trace inequality (3.9) implies

$$\|h^{1/2}(\boldsymbol{q} - R_h \boldsymbol{q})\|_{\mathcal{F}} \lesssim \|\boldsymbol{q} - R_h \boldsymbol{q}\| + h \|\nabla(\boldsymbol{q} - R_h \boldsymbol{q})\|,$$

which, combining with the approximation properties, gives

$$\|\mu(v - i_h v)\| + \|h^{\frac{1}{2}}(\boldsymbol{q} - R_h \boldsymbol{q})\|_{\mathcal{F}} + \|\boldsymbol{q} - R_h \boldsymbol{q}\| \lesssim |\mu| h^{k+1} |v|_{H^{k+1}(\Omega)} + h^{l+1} |\boldsymbol{q}|_{H^{l+1}(\Omega)}.$$

(3.16) is then a direct consequence of the above inequality and (3.17). This completes the proof of the lemma. ∎

To facilitate the analysis we rewrite the system (3.12)–(3.13) in the following compact form: finding $(u_h, \boldsymbol{p}_h, z_h) \in V^k_{g,D} \times RT^l_{\psi,N} \times X^m_h$ such that

$$\mathcal{A}[(u_h, \boldsymbol{p}_h, z_h), (v_h, \boldsymbol{q}_h, x_h)] = l_h(x_h), \quad \forall\, (v_h, \boldsymbol{q}_h, x_h) \in V^k_{0,D} \times RT^l_{0,N} \times X^m_h, \tag{3.18}$$

where

$$\mathcal{A}[(u_h, \boldsymbol{p}_h, z_h), (v_h, \boldsymbol{q}_h, x_h)] = b(\boldsymbol{q}_h, v_h, z_h) + b(\boldsymbol{p}_h, u_h, x_h) + s[(u_h, \boldsymbol{p}_h), (v_h, \boldsymbol{q}_h)],$$

and

$$l_h(x_h) = (f, x_h).$$

Note that for the exact solution, $(u, \boldsymbol{p})$, there holds

$$\mathcal{A}[(u, \boldsymbol{p}, 0), (v_h, \boldsymbol{q}_h, x_h)] = l(x_h). \tag{3.19}$$

PROPOSITION 3.2 (Inf-sup Condition). *Let $k = l = m$ in (3.18). Then there exists $\alpha_c > 0$ such that, for all $(v_h, \boldsymbol{q}_h, x_h) \in V^k_{0,D} \times RT^k_{0,N} \times X^k_h$, there exists $(\tilde{v}_h, \tilde{\boldsymbol{q}}_h, \tilde{x}_h) \in V^k_{0,D} \times RT^k_{0,N} \times X^k_h$ satisfying*

$$\alpha_c(|||(v_h, \boldsymbol{q}_h)|||^2_{-1} + \|x_h\|^2_{1,h}) \leq \mathcal{A}[(v_h, \boldsymbol{q}_h, x_h), (\tilde{v}_h, \tilde{\boldsymbol{q}}_h, \tilde{x}_h)] \tag{3.20}$$

and

$$|||(\tilde{v}_h, \tilde{\boldsymbol{q}}_h)|||_{-1} + \|\tilde{x}_h\|_{1,h} \lesssim |||(v_h, \boldsymbol{q}_h)|||_{-1} + \|x_h\|_{1,h}. \tag{3.21}$$

Proof. Define $\boldsymbol{\eta}_h = \boldsymbol{\eta}_h(x_h) \in RT^k_{0,N}$ by taking $l = m = k$ in (3.5)–(3.6) and $\xi_h := h^2(\nabla \cdot \boldsymbol{q}_h + \mu v_h) \in X^k_h$. We claim that, by choosing $\tilde{v}_h = v_h \in V^k_{0,D}$, $\tilde{\boldsymbol{q}}_h = \boldsymbol{q}_h + \epsilon\boldsymbol{\eta}_h \in RT^k_{0,N}$ and $\tilde{x}_h = -x_h + \xi_h \in X^k_h$, there holds (3.20) and (3.21), where ϵ is to be determined later.

By the above definitions, we have

$$\begin{aligned} &\mathcal{A}[(v_h, \boldsymbol{q}_h, x_h), (v_h, \boldsymbol{q}_h + \epsilon\boldsymbol{\eta}_h, -x_h + \xi_h)] \\ &= \|\boldsymbol{q}_h - \boldsymbol{\beta} v_h + A\nabla v_h\|^2 + \|h(\nabla \cdot \boldsymbol{q}_h + \mu v_h)\|^2 \\ &\quad + \epsilon(\boldsymbol{q}_h - \boldsymbol{\beta} v_h + A\nabla v_h, \boldsymbol{\eta}_h) + \epsilon(\nabla \cdot \boldsymbol{\eta}_h, x_h). \end{aligned} \tag{3.22}$$

For the last term, it follows from integration by parts, (3.5), (3.6) and the facts that $\boldsymbol{\eta}_h \cdot \boldsymbol{n} = 0$ on Γ_N, $\nabla x_h|_K \in \mathbb{P}_{k-1}(K)^d$ and $x_h|_F \in \mathbb{P}^k(F)$ that

$$(\nabla \cdot \boldsymbol{\eta}_h, x_h) = \sum_{K\in\mathcal{T}} (-(\boldsymbol{\eta}_h, \nabla x_h)_K + \langle \boldsymbol{\eta}_h \cdot \boldsymbol{n}_K, x_h\rangle_{\partial K}) = \|\nabla x_h\|^2 + \sum_{F\in\mathcal{F}_I\cup\mathcal{F}_D} \|h^{-\frac{1}{2}}[\![x_h]\!]\|^2_F,$$

which, combining with (3.22), the Cauchy-Schwartz inequality and (3.7), gives

$$\begin{aligned} &\mathcal{A}[(v_h, \boldsymbol{q}_h, x_h), (v_h, \boldsymbol{q}_h + \epsilon\boldsymbol{\eta}_h, -x_h + \xi_h)] \\ &\geq \|\boldsymbol{q}_h - \boldsymbol{\beta} v_h + A\nabla v_h\|^2 + \|h(\nabla \cdot \boldsymbol{q}_h + \mu v_h)\|^2 - \frac{1}{4}\|\boldsymbol{q}_h - \boldsymbol{\beta} v_h + A\nabla v_h\|^2 \\ &\quad - \epsilon^2\|\boldsymbol{\eta}_h\|^2 + \epsilon\left(\|\nabla x_h\|^2 + \sum_{F\in\mathcal{F}_I\cup\mathcal{F}_D} \|h^{-\frac{1}{2}}[\![x_h]\!]\|^2_F\right) \\ &\geq \frac{3}{4}\|\boldsymbol{q}_h - \boldsymbol{\beta} v_h + A\nabla v_h\|^2 + \|h(\nabla \cdot \boldsymbol{q}_h + \mu v_h)\|^2 + \epsilon(1 - \epsilon C^2_{ds})\|x_h\|^2_{1,h}. \end{aligned} \tag{3.23}$$

(3.20) is then a direct result of (3.23) by choosing $\epsilon = \frac{1}{2}C^{-2}_{ds}$ and $\alpha_c = \min\left(\frac{3}{4}, \frac{1}{2}\epsilon\right)$.

To prove (3.21) first applying the triangle inequality gives

$$|||(\tilde{v}_h, \tilde{\boldsymbol{q}}_h)|||_{-1} + \|\tilde{x}_h\|_{1,h} \leq |||(v_h, \boldsymbol{q}_h)|||_{-1} + \|x_h\|_{1,h} + |||(0, \epsilon\boldsymbol{\eta}_h)|||_{-1} + \|\xi_h\|_{1,h}, \tag{3.24}$$

Then applying the trace and inverse inequalities and (3.7) yields

$$|||(0, \epsilon\boldsymbol{\eta}_h)|||_{-1} = \epsilon(\|\boldsymbol{\eta}_h\| + \|h\nabla \cdot \boldsymbol{\eta}_h\|) \lesssim \|\boldsymbol{\eta}_h\| \lesssim \|x_h\|_{1,h}, \tag{3.25}$$

and

$$\|\xi_h\|_{1,h} \lesssim h^{-1}\|\xi_h\| = \|h(\nabla \cdot \boldsymbol{q}_h + \mu v_h)\| \leq |||v_h, \boldsymbol{q}_h|||_{-1}. \tag{3.26}$$

Combining (3.24)–(3.26) results in (3.21). This completes the proof of the proposition. ∎

PROPOSITION 3.3 (Existence and Uniqueness). *The linear system defined by* (3.18) *admits an unique solution* $(u_h, \boldsymbol{p}_h, z_h) \in V^k_{g,D} \times RT^k_{\psi,N} \times X^k_h$.

Proof. In order to prove the invertibility of the square linear system it is equivalent to prove the uniqueness. Assume that there exist two sets of solutions, $(u_{1,h}, \boldsymbol{p}_{1,h}, z_{1,h})$ and $(u_{2,h}, \boldsymbol{p}_{2,h}, z_{2,h})$, both in $V^k_{g,D} \times RT^k_{\psi,N} \times X^k_h$. We then have that for all $(v_n, \boldsymbol{q}_h, x_h)$ in the space of $V^k_{0,D} \times RT^k_{0,N} \times X^k_h$ there holds

$$\mathcal{A}[(u_{1,h} - u_{2,h}, \boldsymbol{p}_{1,h} - \boldsymbol{p}_{2,h}, z_{1,h} - z_{2,h}), (v_h, \boldsymbol{q}_h, x_h)] = 0.$$

By Proposition 3.2, the following must be true:

$$\|(u_{1,h}-u_{2,h},\boldsymbol{p}_{1,h}-\boldsymbol{p}_{2,h})\|_{-1}+\|z_{1,h}-z_{2,h}\|_{1,h}=0,$$

which immediately implies

$$z_{1,h}=z_{2,h}\quad\text{and}\quad\nabla\cdot(\boldsymbol{\beta}(u_{1,h}-u_{2,h})-A\nabla(u_{1,h}-u_{2,h}))+\mu(u_{1,h}-u_{2,h})=0.$$

Since (2.1)–(2.2) admits an unique trivial solution for zero datum we conclude that $u_{1,h}=u_{2,h}$ and, hence, $\boldsymbol{p}_{1,h}=\boldsymbol{p}_{2,h}$. This completes the proof of the proposition. ∎

We end this section by proving the continuity of the bilinear form.

PROPOSITION 3.4 (Continuity). *For all $(v,\boldsymbol{q})\in H^1(\Omega)\times H_{0,N}(div,\Omega)$ and for all $(v_h,\boldsymbol{q}_h,x_h)\in V_h^k\times RT^l\times X_h^m$ there holds*

$$\mathcal{A}[(v,\boldsymbol{q},0),(v_h,\boldsymbol{q}_h,x_h)]\leq|||(v,\boldsymbol{q})|||_\sharp\,(|||(v_h,\boldsymbol{q}_h)|||_{-1}+\|x_h\|_{1,h}).\tag{3.27}$$

Proof. The inequality (3.27) follows by first using the Cauchy-Schwarz inequality in the symmetric part of the formulation,

$$s[(v,\boldsymbol{q}),(v_h,\boldsymbol{q}_h)]\lesssim s[(v,\boldsymbol{q}),(v,\boldsymbol{q})]^{\frac{1}{2}}s[(v_h,\boldsymbol{q}),(v_h,\boldsymbol{q})]^{\frac{1}{2}}.$$

For the remaining term we use the divergence formula elementwisely to obtain

$$(\nabla\cdot\boldsymbol{q}+\mu v,x_h)=\sum_{K\in\mathcal{T}}-(\boldsymbol{q},\nabla x_h)_K+\sum_{F\in\mathcal{F}_I\cup\mathcal{F}_D}\langle\boldsymbol{q}\cdot\boldsymbol{n}_F,[\![x_h]\!]\rangle_F+(\mu v,x_h).$$

(3.27) then follows by applying the Cauchy-Schwartz inequality and (3.4). This completes the proof of the proposition. ∎

4. Error Estimation. In this section we will prove optimal error estimates for smooth solutions, both in the diffusion dominated and the advection dominated regimes. When the diffusion dominates we prove optimal error estimates in both the H^1- and L^2-norms under very mild stability assumptions on the continuous problem. In this part constants may blow up as the Peclet number becomes large.

For dominating advection we need to make an assumption on the problem data to prove an error estimate in the H^{-1}-norm. This is then used to prove an estimate that is optimal for the error in the divergence of the flux, computed using the primal variable, or the "streamline derivative". However, we can not improve on the order for the L^2-error as for typical residual based stabilized finite element methods. In this part constants remain bounded as the Peclet number becomes high.

4.1. Error estimate for the residual. First we prove the optimal convergence result for the residual, i.e., the optimal convergence for the triple norm (3.14). This estimate will then be of use in both the high and low Peclet regimes.

LEMMA 4.1 (Estimate of Residual). *Assume that $(u,\boldsymbol{p})$ is the solution to (2.4) with $u\in H^{k+1}\cap V_{g,D}(\Omega)$, $\boldsymbol{p}\in H^{l+1}(\Omega)^d\cap H_{\psi,N}(\Omega)^d$ and $l\leq k$, and that $(u_h,\boldsymbol{p}_h,z_h)\in V_{g,D}^k\times RT_{\psi,N}^k\times X_h^k$ is the solution of (3.18). Then there holds*

$$|||(u-u_h,\boldsymbol{p}-\boldsymbol{p}_h)|||_{-1}+\|z_h\|_{1,h}\lesssim c_u h^k|u|_{H^{k+1}(\Omega)}+h^{l+1}|\boldsymbol{p}|_{H^{l+1}(\Omega)}.\tag{4.1}$$

Proof. Firstly, applying the triangle inequality gives

$$|||(u-u_h,\boldsymbol{p}-\boldsymbol{p}_h)|||_{-1}\leq|||(u-i_hu,\boldsymbol{p}-R_h\boldsymbol{p})|||_{-1}+|||(u_h-i_hu,\boldsymbol{p}_h-R_h\boldsymbol{p})|||_{-1}.\tag{4.2}$$

Note that $u_h - i_h u \in V_{0,D}^k$ and $\boldsymbol{p}_h - R_h\boldsymbol{p} \in RT_{0,N}^k$. Then by Proposition 3.2 there exists $(v_h, \boldsymbol{q}_h, w_h) \in V_{0,D}^k \times RT_{0,N}^k \times X_h^k$ such that

$$
\begin{aligned}
&|||(u_h - i_h u, \boldsymbol{p}_h - R_h\boldsymbol{p})|||_{-1}^2 + \|z_h\|_{1,h}^2 \\
&\lesssim \mathcal{A}[(u_h - i_h u, \boldsymbol{p}_h - R_h\boldsymbol{p}, z_h)), (v_h, \boldsymbol{q}_h, w_h)] = \mathcal{A}[(u - i_h u, \boldsymbol{p} - R_h\boldsymbol{p}, 0), (v_h, \boldsymbol{q}_h, w_h)] \\
&\lesssim |||(u - i_h u, \boldsymbol{p} - R_h\boldsymbol{p})|||_\sharp \left(|||(u_h - i_h u, \boldsymbol{p}_h - R_h\boldsymbol{p})|||_{-1} + \|z_h\|_{1,h}\right).
\end{aligned}
$$

The last equality and inequality follows from (3.18), (3.19) and Proposition 3.4. Therefore, we immediately have that

$$
|||(u_h - i_h u, \boldsymbol{p}_h - R_h\boldsymbol{p})|||_{-1} \lesssim |||(u - i_h u, \boldsymbol{p} - R_h\boldsymbol{p})|||_\sharp
$$

which, combing with (3.16) and (4.2), implies (4.1). This completes the proof of the lemma. ∎

Observe that the hidden constant in (4.1) has no inverse powers of the diffusivity. Hence we have the following corollary.

COROLLARY 4.1. *Under the same assumptions as in Lemma 4.1, if* $\|A\|_\infty << h$, $\boldsymbol{\beta}_\infty = O(1)$, $|\mu| = O(1)$, *there holds*

$$
|||(u - u_h, \boldsymbol{p} - \boldsymbol{p}_h)|||_{-1} + \|z_h\|_{1,h} \lesssim h^{k+1}|u|_{H^{k+1}(\Omega)} + h^{l+1}|\boldsymbol{p}|_{H^{l+1}(\Omega)}. \tag{4.3}
$$

4.2. Error estimates in the diffusion dominated regime. In this subsection we provide results for the error estimation in the diffusion dominated regime, i.e., $\dfrac{\boldsymbol{\beta}_\infty}{\lambda_{min,A}}$ is of order 1 where $\lambda_{min,A}$ is the smallest eigenvalue of A.

PROPOSITION 4.1 (H^1-norm estimate). *Assume that* $(u, \boldsymbol{p})$ *is the solution to* (2.4), $u \in H^{k+1}(\Omega) \cap V_{g,D}(\Omega)$ *and* $\boldsymbol{p} \in H^{l+1}(\Omega)^d \cap H_{\psi,N}(\Omega)^d$ *with* $l < k$, *and that* $(u_h, \boldsymbol{p}_h)$ *is the solution of* (3.18). *Then the following estimate holds,*

$$
\|u - u_h\|_V \leq C\left(c_u h^k |u|_{H^{k+1}(\Omega)} + h^{l+1}\left(|\boldsymbol{p}|_{H^{l+1}(\Omega)} + |\psi|_{H^{l+1/2}(\Gamma_N)}\right)\right), \tag{4.4}
$$

where the constant C *depends on the datum in the following manner*

$$
C \equiv \frac{\|\boldsymbol{\beta}\|_\infty}{\lambda_{min,A}}.
$$

REMARK 4.1. *Since the above constant* C *blows up as* $\lambda_{min,A}$ *goes to zero, the above estimation is valid only for diffusion dominated problem.*

Proof. To avoid using coercivity arguments, our starting point for the error analysis below is the stability estimate (2.5). Let $e = u - u_h$. we note that e is a solution to (2.4) with the right hand side linear operator being $r(v) := l(v) - a(u_h, v)$, i.e.,

$$
a(e, v) = r(v).
$$

Now apply the decomposition $e = e_0 + e_g$ such that $e_g|_{\Gamma_D} = e|_{\Gamma_D}$ and that $\|e_g\|_V \lesssim \|e\|_{H^{1/2}(\Gamma_D)}$. It then follows from (2.5) that

$$
\|e_0\|_V \leq C \sup_{v \in V} \frac{r(v) - a(e_g, v)}{\|v\|_V} \leq C(\|r\|_{V'} + \|e_g\|_V).
$$

Hence

$$\|e\|_V \le \|e_0\|_V + \|e_g\|_V \le C(\|r\|_{V'} + \|e_g\|_V).$$

For the term $\|e_g\|_V$, by definition and a standard trace inequality, we have

$$\|e_g\|_V \le C\|u - i_h u\|_{H^{\frac{1}{2}}(\Gamma_D)} \le C\|u - i_h u\|_V \le Ch^k |u|_{H^{k+1}(\Omega)}. \tag{4.5}$$

To prove the bound on $\|r\|_{V'}$ we recall that

$$\|r\|_{V'} = \sup_{v\in V} \frac{a(u-u_h, v)}{\|v\|_V}.$$

Then by integration by parts, (3.13) and Cauchy Schwartz inequality, we have

$$\begin{aligned}
&a(u-u_h, v) = l(v) - a(u_h, v)\\
&= (f, v) + (\psi, v)_{\Gamma_N} - (A\nabla u_h - \beta u_h, \nabla v) - (\mu u_h, v)\\
&= (f - \nabla\cdot \boldsymbol{p}_h - \mu u_h, v) + (\psi + \boldsymbol{p}_h\cdot n, v)_{\Gamma_N} - (\boldsymbol{p}_h - \beta u_h + A\nabla u_h, \nabla v)\\
&= (f - \nabla\cdot \boldsymbol{p}_h - \mu u_h, v - \pi_{X,0} v) + (\boldsymbol{p} - \boldsymbol{p}_h - \beta(u-u_h) + A\nabla(u-u_h), \nabla v)\\
&\quad +(\psi - \psi_h, v - \pi_{F,0} v)_{\Gamma_N}\\
&\lesssim |||(\boldsymbol{p} - \boldsymbol{p}_h), (u-u_h)|||_{-1} \|\nabla v\| + \|h^{\frac{1}{2}}(\psi - \psi_h)\|_{\Gamma_N} \|\nabla v\|
\end{aligned}$$

which, combining with (4.5), (4.1) and the following observation (see e.g., Lemma 5.2 of [29])

$$\|h^{\frac{1}{2}}(\psi - \psi_h)\|_{\Gamma_N} \lesssim h^{l+1} |\psi|_{H^{l+1/2}(\Gamma_N)},$$

gives (4.4). This completes the proof of the proposition. ∎

In the remaining part of this subsection we will focus on the convergence of the L^2-norm error in the primal variable. For simplicity we here restrict the discussion to the case of a convex polygonal domain Ω and homogeneous Dirichlet condition. We first prove the convergence result for the L^2-norm of the Lagrange multiplier.

PROPOSITION 4.2. *Assume that $u \in H_0^1(\Omega) \cap H^{k+1}(\Omega)$ and $\boldsymbol{p} \in H^k(\Omega)^d$. Let z_h be the Lagrange multiplier of the system (3.18). We have the following error estimate*

$$\|z_h\|_\Omega \lesssim h^{k+1} \left(|u|_{H^{k+1}(\Omega)} + |\boldsymbol{q}|_{H^k(\Omega)} \right). \tag{4.6}$$

Proof. Let ϕ be the solution such that

$$\nabla\cdot(\boldsymbol{\beta}\phi - A\nabla\phi) + \mu\phi = z_h$$

with boundary condition $\phi = 0$ on $\partial\Omega$. Then by the well-posedness assumption on the equation (2.1) and the assumption on Ω we have the following stability result:

$$\|\phi\|_{H^2(\Omega)} \lesssim \|z_h\|. \tag{4.7}$$

Let $\boldsymbol{q} = \boldsymbol{\beta}\phi - A\nabla\phi$. By adding and subtracting suitable interpolates we have

$$\|z_h\|^2 = (z_h, \nabla\cdot(\boldsymbol{q} - R_h\boldsymbol{q}) + \mu(\phi - i_h\phi)) + (z_h, \nabla\cdot R_h\boldsymbol{q} + \mu i_h\phi). \tag{4.8}$$

For the first term in (4.8) using the element-wise divergence theorem, the facts that

$$\int_F z_h(\boldsymbol{q} - R_h\boldsymbol{q})\cdot \boldsymbol{n}_K \, ds = 0, \quad \forall K \in \mathcal{T}, \forall F \subset \partial K,$$

and that

$$\|\boldsymbol{q} - R_h\boldsymbol{q}\| \lesssim h\|\phi\|_{H^2(\Omega)} \lesssim h\|z_h\| \quad \text{and} \quad \|\phi - i_h\phi\| \lesssim h^2\|\phi\|_{H^2(\Omega)} \lesssim h^2\|z_h\|,$$

and (3.4) gives

$$(z_h, \nabla\cdot(\boldsymbol{q} - R_h\boldsymbol{q}) + \mu(\phi - i_h\phi)) \lesssim h(1 + \|\mu\|_\infty h)\|z_h\|_{1,h}\|z_h\|. \tag{4.9}$$

For the second term in (4.8) we first apply equation (3.12) with $\boldsymbol{q}_h = R_h(\boldsymbol{q}) \in RT^k$ and $v_h = i_h\varphi \in V^k_{0,D}$ with $\Gamma_N = \emptyset$, then applying the Cauchy-Schwarz inequality, (3.1) and (3.2) that

$$\begin{aligned}
&(z_h, \nabla\cdot R_h\boldsymbol{q} + \mu i_h\phi) = -(\boldsymbol{p}_h - \boldsymbol{\beta}u_h + A\nabla u_h, R_h\boldsymbol{q} - \boldsymbol{\beta}i_h\phi + A\nabla(i_h\phi))\\
\lesssim&\|\boldsymbol{p}_h - \boldsymbol{\beta}u_h + A\nabla u_h\|\left(\|A\|_\infty\|\nabla(\phi - i_h\phi)\| + \|\boldsymbol{\beta}\|_\infty\|\phi - i_h\phi\| + \|\boldsymbol{q} - R_h\boldsymbol{q}\|\right)\\
\lesssim&\|(\boldsymbol{p}_h - \boldsymbol{\beta}u_h + A\nabla u_h)\|\left(\|A\|_\infty h + \|\boldsymbol{\beta}\|_\infty h^2 + h\right)\|\phi\|_{H^2(\Omega)}\\
\lesssim&h\|(\boldsymbol{p}_h - \boldsymbol{\beta}u_h + A\nabla u_h)\|\|z_h\|.
\end{aligned} \tag{4.10}$$

(4.6) is then a direct consequence of (4.9), (4.10) and (4.1). This completes the proof of the proposition. ∎

We now proceed to prove the error estimation of the primal variable in the L^2 norm. To estimate the error of the primal variable in the L^2 norm we require that the adjoint problem is well-posed and satisfies a shift theorem for the H^2 semi-norm.

Assumption 4.1. *Consider the adjoint problem for (2.1). For each $\zeta \in L^2(\Omega)$, we assume that the data are such that the following adjoint problem admits an unique solution, using Fredholm's alternative,*

$$-\nabla\cdot A\nabla\varphi - \boldsymbol{\beta}\cdot\nabla\varphi + \mu\varphi = \zeta \text{ in } \Omega \tag{4.11}$$

with $\varphi|_{\partial\Omega} = 0$. Furthermore, the following regularity result holds true:

$$\|\varphi\|_{H^2(\Omega)} \lesssim \|\zeta\|. \tag{4.12}$$

Proposition 4.3. *Let $u \in H^{k+1}(\Omega) \cap H^1_0(\Omega)$, $\boldsymbol{p} \in H^k(\Omega)^d$ and $(u_h, \boldsymbol{p}_h, z_h)$ be the solution of (3.12)–(3.13). Under the Assumption 4.1 we have*

$$\|u - u_h\| \lesssim h^{k+1}\left(|u|_{H^{k+1}(\Omega)} + |\boldsymbol{p}|_{H^k(\Omega)}\right). \tag{4.13}$$

Proof. Let φ be the solution of the dual problem (4.11) with right hand side being $e := u - u_h$. Then by integration by parts, the assumption that $\varphi = 0$ on $\partial\Omega$, we have

$$\begin{aligned}
\|e\|^2 &= (f, \varphi) + (u_h, \nabla\cdot A\nabla\varphi + \boldsymbol{\beta}\cdot\nabla\varphi - \mu\varphi)\\
&= (f - \nabla\cdot\boldsymbol{p}_h - \mu u_h, \varphi) - (\boldsymbol{p}_h + A\nabla u_h - \boldsymbol{\beta}u_h, \nabla\varphi).
\end{aligned} \tag{4.14}$$

The first term can be estimated by applying (3.13) and the Cauchy-Schwartz inequality:

$$(f - \nabla\cdot\boldsymbol{p}_h - \mu u_h, \varphi) = (f - \nabla\cdot\boldsymbol{p}_h - \mu u_h, \varphi - \pi_{X,k}\varphi) \lesssim h|||(u - u_h, \boldsymbol{p} - \boldsymbol{p}_h)|||_{-1}\|\varphi\|_{H^2(\Omega)}. \tag{4.15}$$

To estimate the second term we apply (3.12) with $\boldsymbol{q}_h = R_h(\nabla\varphi) \in RT^k$ and the fact that $\nabla\cdot(R_h\nabla\varphi)) = \pi_{X,k}\triangle\varphi$:

$$\begin{aligned}
&(\boldsymbol{p}_h + A\nabla u_h - \boldsymbol{\beta}u_h, \nabla\varphi)\\
=&-(z_h, \nabla\cdot(R_h\nabla\varphi)) + (\boldsymbol{p}_h + A\nabla u_h - \boldsymbol{\beta}u_h, (\nabla\varphi - R_h\nabla\varphi))\\
\lesssim&\|z_h\|\|\pi_{X,k}\triangle\varphi\| + h\|\boldsymbol{p}_h + A\nabla u_h - \boldsymbol{\beta}u_h\|\|\varphi\|_{H^2(\Omega)}\\
\lesssim&(\|z_h\| + h\|\boldsymbol{p}_h + A\nabla u_h - \boldsymbol{\beta}u_h\|)\|\varphi\|_{H^2(\Omega)}.
\end{aligned} \tag{4.16}$$

Combing (4.14)–(4.16) gives

$$\|e\| \lesssim h|||(u-u_h, \boldsymbol{p}-\boldsymbol{p}_h)|||_{-1} + \|z_h\|. \tag{4.17}$$

(4.13) is then a direct consequence of (4.17), (4.1) and (4.6). This completes the proof of the proposition. ∎

REMARK 4.2. *Observe that the hidden constants in (4.7) and (4.12) typically blow up in the advection dominated regime. Therefore the above L^2-analysis is relevant only in the low Peclet regime.*

4.3. Error estimates in the advection dominated regime. In this section, we analyze the error estimates in the advection dominated regime. For the stability we make the following assumption on the data that ensures stability of the adjoint equation independent of the diffusivity, see [24].

ASSUMPTION 4.2. *We assume that the the domain Ω is convex, that the diffusivity A is a scalar and $\boldsymbol{\beta}_\infty = O(1)$. We also introduce the following condition on data. Let $\mathcal{I}$ denote the identity matrix and $\nabla_S \boldsymbol{\beta} := 1/2(\nabla\boldsymbol{\beta} + (\nabla\boldsymbol{\beta})^T)$, i.e., the symmetric part of $\nabla\boldsymbol{\beta}$. Then assume that $\mu\mathcal{I} - (\nabla_S\boldsymbol{\beta} - \frac{1}{2}\nabla\cdot\boldsymbol{\beta}\mathcal{I})$ is symmetric positive definite and denote by Λ_{min} its smallest eigenvalue. Moreover we assume that $\boldsymbol{\beta}\cdot\boldsymbol{n} = 0$ on $\partial\Omega$.*

We first prove the following inverse inequality regarding the $H^{-1}(\Omega)$ norm.

LEMMA 4.2. *For any $v_h \in V_h^k$ the following inverse inequality holds:*

$$\|v_h\|_{L^2(\Omega)} \lesssim h^{-1}\|v_h\|_{H^{-1}(\Omega)} \tag{4.18}$$

Proof. Let $E \in H_0^1(\Omega)$ be the weak solution to

$$-\triangle E + E = v_h \text{ in } \Omega.$$

Then by the definition and duality inequality we have

$$\begin{aligned} \|E\|_{H^1(\Omega)} &= \sup_{\substack{w\in H_0^1(\Omega)\\ \|w\|_{H^1(\Omega}=1}} ((\nabla E, \nabla w) + (E, w)) \\ &= \sup_{\substack{w\in H_0^1(\Omega)\\ \|w\|_{H^1(\Omega)}=1}} (-\triangle E + E, w) \le \|v_h\|_{H^{-1}(\Omega)}. \end{aligned} \tag{4.19}$$

By integration by parts we also have

$$\|v_h\|^2 = (v_h, -\triangle E + E) = (v_h, E) + (\nabla v_h, \nabla E) \le \|v_h\|_{H^1(\Omega)}\|E\|_{H^1(\Omega)},$$

which, combining with (4.19) and the inverse inequality, gives (4.18). This completes the proof of the lemma. ∎

LEMMA 4.3. *Let $\phi \in H_0^1(\Omega)$ be the solution to (4.11) with the right side being $\psi \in H_0^1(\Omega)$. Then under the Assumption 4.2 the following stability result holds:*

$$\Lambda_{min}\|\nabla\phi\| \le \|\nabla\psi\|. \tag{4.20}$$

Proof. By the definition and integration by parts we have

$$(\psi, -\triangle\phi) = (\mu\nabla\phi, \nabla\phi) + (\boldsymbol{\beta}\cdot\nabla\phi, \triangle\phi) + (A\triangle\phi, \triangle\phi)$$

Using the relation of [10, equation (3.6)] we have for the second term of the right hand side

$$(\boldsymbol{\beta}\cdot\nabla\phi,\triangle\phi) = \left(\left(\frac{1}{2}\nabla\cdot\boldsymbol{\beta}\mathcal{I} - \nabla_S\boldsymbol{\beta}\right)\nabla\phi,\nabla\phi\right). \tag{4.21}$$

Combining similar terms we then have

$$\left(\left(\mu\mathcal{I} - (\nabla_S\boldsymbol{\beta} - \frac{1}{2}\nabla\cdot\boldsymbol{\beta}\mathcal{I})\right)\nabla\phi,\nabla\phi\right) + (A\triangle\phi,\triangle\phi) = (\psi,-\triangle\phi) = (\nabla\psi,\nabla\phi), \tag{4.22}$$

and, therefore,

$$\Lambda_{min}\|\nabla\phi\| \leq \|\nabla\psi\| \tag{4.23}$$

and, as a by product,

$$\|A^{1/2}D^2\phi\| \lesssim \|A^{1/2}\triangle\phi\| \leq \Lambda_{min}^{-1/2}\|\nabla\psi\|.$$

This completes the proof of the lemma. ∎

Proposition 4.4. *Let u and u_h be the solution of (2.4) and (3.18), respectively. Then under the Assumption 4.2 we have the following estimate:*

$$\|u-u_h\|_{H^{-1}(\Omega)} \leq C_P\Lambda_{min}^{-1}|||u-u_h,\boldsymbol{p}-\boldsymbol{p}_h||| \tag{4.24}$$

where C_P is the constant of the Poincaré inequality

$$\sum_K \|h_K^{-1}(\phi-\pi_{X,0}\phi)\|^2 \leq C_P^2\|\nabla\phi\|^2$$

and Λ_{min} is defined in Assumption 4.2. $C_P = \pi^{-1}$ on convex domains, see [?].

Proof. By definition we have

$$\|u-u_h\|_{H^{-1}(\Omega)} = \sup_{\substack{w\in H_0^1(\Omega)\\ \|w\|_{H^1(\Omega)}=1}} (e_u,w).$$

Let $\varphi\in H_0^1(\Omega)$ be the solution of (4.11) with the right hand side an arbitrary function $\psi\in H_0^1(\Omega)$ with $\|\psi\|_{H^1(\Omega)}=1$. Applying the integration by parts, (3.13) and the Cauchy-Schwartz inequality gives

$$\begin{aligned}
(e_u,\psi) &= (e_u,\mu\varphi - \boldsymbol{\beta}\cdot\nabla\varphi - A\triangle\varphi)\\
&= (\mu e_u + \nabla\cdot\boldsymbol{e}_p,\varphi) + (\boldsymbol{e}_p + A\nabla e_u - \boldsymbol{\beta}e_u,\nabla\varphi)\\
&= (\mu e_u + \nabla\cdot\boldsymbol{e}_p,\varphi-\pi_{X,0}\varphi) + (\boldsymbol{e}_p + A\nabla e_u - \boldsymbol{\beta}e_u,\nabla\varphi)\\
&\leq (C_P\|h(\mu e_u + \nabla\cdot\boldsymbol{e}_p)\| + \|\boldsymbol{e}_p + A\nabla e_u - \boldsymbol{\beta}e_u\|)\,\|\nabla\varphi\|\\
&\leq C_P|||(u-u_h,\boldsymbol{p}-\boldsymbol{p}_h)|||_{-1}\|\nabla\varphi\| \leq C_P\Lambda_{min}^{-1}|||(u-u_h,\boldsymbol{p}-\boldsymbol{p}_h)|||_{-1}.
\end{aligned}$$

where in the last inequality we also applied the stability result of Lemma 4.3. This completes the proof of the proposition, since the bound is valid for arbitrary $\psi\in H_0^1(\Omega)$ with $\|\psi\|_{H^1(\Omega)}=1$. ∎

COROLLARY 4.2 (Negative norm, a posteriori and a priori bounds). *Under the same hypothesis as Proposition 4.4 the following a posteriori and a priori error estimates hold:*

$$\begin{aligned}\|u-u_h\|_{H^{-1}(\Omega)} &\leq C_P\Lambda_{min}^{-1}(\|h(f-\mu u_h-\nabla\cdot\boldsymbol{p}_h)\|+\|\boldsymbol{\beta}u_h-A\nabla u_h-\boldsymbol{p}_h\|)\\ &\lesssim C_P\Lambda_{min}^{-1}(h^{k+1}|u|_{H^{k+1}(\Omega)}+h^{l+1}|\boldsymbol{p}|_{H^{l+1}(\Omega)})\end{aligned}\tag{4.25}$$

Proof. The proof is immediate using Proposition 4.4 and Corollary 4.1. ∎

We are now ready to prove the main result.

THEOREM 4.1. *Let $u\in H^{k+1}(\Omega)\cap H_0^1(\Omega)$, $\boldsymbol{p}\in H^{k+1}(\Omega)^d$ and $(u_h,\boldsymbol{p}_h,z_h)$ be the solution of (3.12)–(3.13). Assume that $A\lesssim h^2$. Then under the Assumption 4.2 we have the following error estimate:*

$$\|u-u_h\|+\|\nabla\cdot(\boldsymbol{p}-\boldsymbol{p}_h)\|\lesssim h^k\left(|u|_{H^{k+1}(\Omega)}+|\boldsymbol{p}|_{H^{k+1}(\Omega)}\right).\tag{4.26}$$

Furthermore, if $\nabla\cdot\boldsymbol{p}\in H^{k+1}(\Omega)$ we have

$$\|\nabla\cdot\boldsymbol{\beta}(u-u_h)\|\lesssim h^k\left(|u|_{H^{k+1}(\Omega)}+|\boldsymbol{p}|_{H^{k+1}(\Omega)}+|\nabla\cdot\boldsymbol{p}|_{H^{k+1}(\Omega)}\right).\tag{4.27}$$

Here the hidden constants are bounded in the limit as $A\to 0$.

Proof. Applying the triangle inequality, (4.18), (4.24) and Corollary 4.1 gives

$$\begin{aligned}\|u-u_h\| &\leq \|u-i_hu\|+h^{-1}\|u_h-i_hu\|_{H^{-1}(\Omega)}\\ &\lesssim h^{k+1}|u|_{H^{k+1}(\Omega)}+h^{-1}\|u-u_h\|_{H^{-1}(\Omega)}+h^{-1}\|u-i_hu\|_{H^{-1}(\Omega)}\\ &\lesssim h^{k+1}|u|_{H^{k+1}(\Omega)}+h^{-1}\|u-u_h\|_{H^{-1}(\Omega)}+h^{-1}\|u-i_hu\|_{L^2(\Omega)}\\ &\lesssim h^k|u|_{H^{k+1}(\Omega)}+h^{-1}|||(u-u_h,\boldsymbol{p}-\boldsymbol{p}_h)|||\\ &\lesssim h^k\left(|u|_{H^{k+1}(\Omega)}+|\boldsymbol{p}|_{H^{k+1}(\Omega)}\right).\end{aligned}\tag{4.28}$$

Applying the triangle inequality, (4.28) and (4.1) gives

$$\begin{aligned}\|\nabla\cdot(\boldsymbol{p}-\boldsymbol{p}_h)\| &\leq \|\nabla\cdot(\boldsymbol{p}-\boldsymbol{p}_h)+\mu(u-u_h)\|+\|\mu(u-u_h)\|\\ &\lesssim h^{-1}|||(u-u_h,\boldsymbol{p}-\boldsymbol{p}_h)|||+\|\mu(u-u_h)\|\\ &\lesssim h^k\left(|u|_{H^{k+1}(\Omega)}+|\boldsymbol{p}|_{H^{k+1}(\Omega)}\right).\end{aligned}\tag{4.29}$$

(4.26) is then a direct result of (4.28) and (4.29).

To prove (4.27) we first apply the triangle inequality,

$$\|\nabla\cdot(\boldsymbol{\beta}(u-u_h))\|\leq\|\nabla\cdot(\boldsymbol{\beta}(u-i_hu))\|+\|\nabla\cdot(\boldsymbol{\beta}(u_h-i_hu))\|.\tag{4.30}$$

The first term in (4.30) can be easily estimated using (3.1). For the second term in (4.30) applying the triangle and inverse inequalities gives

$$\begin{aligned}\|\nabla\cdot(\boldsymbol{\beta}(u_h-i_hu))\| \leq\ & h^{-1}\|\boldsymbol{\beta}(u_h-i_hu)-(R_h\boldsymbol{p}-\boldsymbol{p}_h)-A\nabla(u_h-i_hu)\|\\ &+h^{-2}\|A\|_\infty\left(\|(u_h-u)\|+\|(i_hu-u)\|\right)\\ &+\|\nabla\cdot(\boldsymbol{p}-\boldsymbol{p}_h)\|+\|\nabla\cdot(\boldsymbol{p}-R_h\boldsymbol{p})\|.\end{aligned}\tag{4.31}$$

By the triangle inequality, Corollary 4.1 and (3.17) we have

$$h^{-1}\|\boldsymbol{\beta}(u_h-i_hu)-(R_h\boldsymbol{p}-\boldsymbol{p}_h)-A\nabla(u_h-i_hu)\|\lesssim h^k(|u|_{H^{k+1}(\Omega)}+|\boldsymbol{p}|_{H^{k+1}(\Omega)}).\tag{4.32}$$

By the smallness assumption $\|A\|_\infty \lesssim h^2$, (3.1), (3.2), (4.28) and (4.29) the remaining terms in (4.31) can be estimated as follows:

$$\begin{aligned} &h^{-2}\|A\|_\infty \left(\|(u_h - u)\| + \|(i_h u - u)\|\right) + \|\nabla \cdot (\boldsymbol{p} - \boldsymbol{p}_h)\| + \|\nabla \cdot (\boldsymbol{p} - R_h \boldsymbol{p})\| \\ &\lesssim h^k \left(|u|_{H^{k+1}(\Omega)} + |\boldsymbol{p}|_{H^{k+1}(\Omega)} + |\nabla \cdot \boldsymbol{p}|_{H^{k+1}(\Omega)}\right). \end{aligned} \tag{4.33}$$

Finally, (4.27) is a direct consequence of (4.30)–(4.33). This completes the proof of the lemma. ∎

Remark 4.1. It is possible to prove Theorem 4.1 under the standard coercivity assumption for advection-diffusion problems, but not Proposition 4.4. Also note that we need the diffusivity to be $O(h^2)$ to ensure that the high Peclet result holds. This is a stronger assumption than is usual for convection–diffusion equations.

5. Numerical Experiments. In this section we present results for numerical experiments in both the diffusion dominated and convection dominated regimes. The numerical results are produced using the FEniCS software [36].

EXAMPLE 5.1 (Boundary Layer). *In this example we consider the boundary layer problem [37]*

$$-\epsilon \triangle u + 2\frac{\partial u}{\partial x} + \frac{\partial u}{\partial y} = f$$

on the domain $\Omega = (-1, 1) \times (-1, 1)$ *where the true solution has the following representation:*

$$u = (1 - \exp(-(1 - x)/\epsilon)) * (1 - \exp(-(1 - y)/\epsilon)) * \cos(\pi(x + y))$$

and $\epsilon \in \mathbb{R}$. *The solution has a* $O(\epsilon)$ *boundary layer along the right top sides of the domain and the value of* ϵ *determines the strength of the boundary layer.*

We first test the value $\epsilon = 1$ in which case the solution is smooth and we aim to test the optimal convergence rates of our method for smooth problems. The magnitude of the errors and their corresponding convergence rates are listed in Table 1 for the first and second orders, i.e., $k = 1$ and $k = 2$. For both orders we observe the optimal convergence performance for the primal variable in both the L^2 and H^1 norms. For the flux variable we are able to observe the optimal rate for the linear order, and, however, a slightly suboptimal rate for the second order. Nevertheless the flux variable provides an approximation of the flux that is more accurate than that using the primal variable by two orders of magnitude.

We then test the method in the advection dominated regime with boundary layer by letting $\epsilon = 0.01$ (see performance results in Table 2). For both the first and second orders, the method produce the optimal convergence rate for the streamline derivative when the layer is resolved. For the flux variable we observe the optimal convergence for both orders 1 and 2 (with even super convergence result for order 2). For the primal variable we observe the optimal convergence rates both in the L^2- and H^1-norms (with super convergence for the L^2- norm in the second order case).

To test the robustness of our method, Figure 1 shows the numerical solutions on structured meshes of various element sizes using the first order method for the problem with $\epsilon = 0.002$ in which case the boundary layer is extremely sharp. More precisely the mesh sizes are chosen such that the boundary layer are under resolved ($h = 1/64$), half resolved ($h = 1/512$) and fully resolved ($h = 1/1024$). We observe that when the mesh size could not resolve the boundary layer fully global oscillations appear in the

TABLE 1
Errors and convergence performance for Example 5.1 with $\epsilon = 1$

h	$\|u - u_h\|$	rate	$\|u - u_h\|_{H^1(\Omega)}$	rate	$\|\boldsymbol{p} - \boldsymbol{p}_h\|$	rate
1/32	1.975E-3	1.99	1.644E-1	1.00	3.346E-3	2.00
1/64	4.942E-4	2.00	8.229E-2	1.00	8.367E-4	2.00
1/128	1.235E-4	2.00	4.115E-2	1.00	2.091E-4	2.00

(a) order =1

h	$\|u - u_h\|$	rate	$\|u - u_h\|_{H^1(\Omega)}$	rate	$\|\boldsymbol{p} - \boldsymbol{p}_h\|$	rate
1/32	1.605E-5	2.99	3.857E-3	2.00	7.368E-5	2.64
1/64	2.008E-6	3.00	9.650E-4	2.00	1.230E-5	2.60
1/128	2.510E-7	3.00	2.412E-4	2.00	2.109E-6	2.54

(b) order =2

TABLE 2
Errors and convergence rates for Example 5.1 with $\epsilon = 0.01$

h	$\|u - u_h\|$	rate	$\|u - u\|_{H^1(\Omega)}$	rate	$\|\boldsymbol{p} - \boldsymbol{p}_h\|$	rate
1/32	1.979E-1	0.86	6.073	0.13	4.394E-1	0.86
1/64	7.195E-2	1.46	4.009	0.60	1.599E-1	1.46
1/128	2.044E-2	1.82	2.189	0.87	4.547E-2	1.81
1/256	5.296E-3	1.95	1.120	0.97	1.178E-2	1.95
h	$\|\nabla \cdot (\boldsymbol{p} - \boldsymbol{p}_h)\|$	rate	$\|\nabla \cdot (\boldsymbol{\beta}(u - u_h))\|$	rate	$\|z_h\|$	rate
1/32	1.277E-0	1.04	9.462	0.09	2.592E-3	1.30
1/64	4.354E-1	1.55	6.314	0.58	7.917E-4	1.71
1/128	1.206E-1	1.85	3.452	0.87	2.092E-4	1.92
1/256	3.100E-2	1.96	1.766	0.97	5.300E-5	1.98

(a) order = 1

h	$\|u - u_h\|$	rate	$\|u - u\|_{H^1(\Omega)}$	rate	$\|\boldsymbol{p} - \boldsymbol{p}_h\|$	rate
1/32	3.461E-2	1.88	2.228E-1	0.87	7.666E-2	1.90
1/64	4.772E-3	2.86	7.838E-1	1.51	1.036E-2	2.89
1/128	4.483E-4	3.41	2.194E-1	1.84	9.210E-4	3.49
1/256	4.186E-5	3.42	5.665E-2	1.95	7.772E-5	3.57
h	$\|\nabla \cdot (\boldsymbol{p} - \boldsymbol{p}_h)\|$	rate	$\|\nabla \cdot (\boldsymbol{\beta}(u - u_h))\|$	rate	$\|z_h\|$	rate
1/32	3.138E-1	1.79	3.505E-0	0.84	3.589E-4	2.10
1/64	5.672E-2	2.47	1.235E-0	1.50	4.582E-5	2.97
1/128	7.992E-3	2.83	3.456E-1	1.84	3.880E-6	3.56
1/256	1.032E-3	2.95	8.919E-2	1.95	2.935E-7	3.72

(b) order=2

approximation solution and jeopardize the quality of the approximations. Observe that the oscillations here are different to those appearing in the standard Galerkin method. In section 6 we propose two simple strategies to tackle this issue.

EXAMPLE 5.2 (Reentrant Corner). *In this example we test a pure diffusion problem, i.e.,* $\epsilon = 1$, $\boldsymbol{\beta} = 0$ *and* $\mu = 0$, *on the L-shaped doman* $\Omega = (-1, 1)^2 \setminus (-1, -1)^2$.

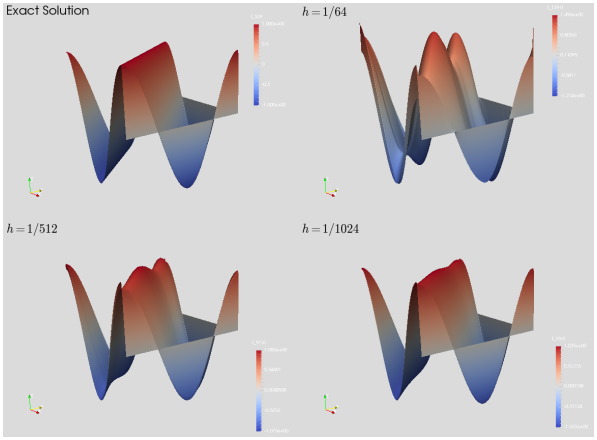


FIG. 1. *Various numerical solutions for Example 5.1 with* $\epsilon = 0.002$

We consider the problem with solution being

$$u(r,\theta) = r^{2/3}\sin(2\theta/3), \quad \theta \in [0, 3\pi/2],$$

in polar coordinates. It is well known that the solution satisfies

$$-\triangle u = 0 \quad in\,\Omega$$

and belongs to $H^{5/3-\epsilon}(\Omega)$ *for* $\epsilon > 0$ *with the singularity located at the reentrant corner, i.e.,* $(0,0)$*. The numerical scheme takes the pure Dirichlet boundary condition.*

TABLE 3
Errors and convergence rates for Example 5.2 with order $= 1$

h	$\|u-u_h\|$	rate	$\|u-u_h\|_{H^1(\Omega)}$	rate	$\|\boldsymbol{p}-\boldsymbol{p}_h\|$	rate
1/16	3.025E-3	1.35	7.790E-2	0.65	4.110E-2	0.67
1/32	1.189E-3	1.35	4.949E-2	0.65	2.589E-2	0.67
1/64	4.689E-4	1.34	3.315E-2	0.66	1.631E-2	0.67

The magnitude of errors and their corresponding convergence rates are presented in Table 3. For this pure diffusion problem, where the solution has singularity and with limited smoothness, we observe the optimal convergence performance for both the primal and flux variables. The flux variable is still a superior approximation of the fluxes, but here only by a factor two.

EXAMPLE 5.3 (Internal Layer). *In this example we consider a pure advection problem [28, Section 5.2.3]. The solution has the following representation:*

$$u(x,y) = exp(-\sigma\rho(x,y)arccos\left(\frac{y+1}{\rho(x,y)}\right)arctan\left(\frac{\rho(x,y)-1.5}{\delta}\right) \tag{5.1}$$

where $\sigma = 0.1$*,* $\rho(x,y) = \sqrt{x^2+(y+1)^2}$*. It is easy to verify that*

$$\nabla\cdot\boldsymbol{\beta} = 0, \quad \boldsymbol{\beta}\cdot\nabla u + \sigma u = 0$$

for $\boldsymbol{\beta} = \dfrac{1}{\rho(x,y)}(y+1, x)$, *and that the inflow boundary,* $\Gamma^- = \{x \in \partial\Omega, \boldsymbol{\beta}(x)\cdot\boldsymbol{n} < 0\}$, *is* $x = 0$ *and* $y = 1$. *The finite element scheme we use for this problem is to find* $u \in V^k_{g,\Gamma^-}$, $\boldsymbol{p} \in RT^k$, *and* $z_h \in X^k_h$ *such that (3.12) and (3.13) hold.*

We first test the case when $\delta = 1$ to test the performance of our method on smooth problems (see performance results in Table 4). We further test the case for $\delta = 0.01$ in which case the solution has a sharp internal layer (see performance results in Table 5).

TABLE 4
Errors and convergence rates for Example 5.3 with $\delta = 1$ *and order* $= 1$

h	$\|u-u_h\|$	rate	$\|u-u\|_{H^1(\Omega)}$	rate	$\|\boldsymbol{p}-\boldsymbol{p}_h\|$	rate
1/32	6.021E-5	2.04	8.591E-3	1.00	6.939E-5	2.03
1/64	1.475E-5	2.03	4.281E-3	1.00	1.711E-5	2.02
1/128	3.638E-6	2.02	2.135E-3	1.00	4.235E-6	2.01
h	$\|\nabla\cdot(\boldsymbol{p}-\boldsymbol{p}_h)\|$	rate	$\|\nabla\cdot(\boldsymbol{\beta}(u-u_h))\|$	rate	$\|z_h\|$	rate
1/32	6.021E-6	2.04	5.343E-3	1.00	1.084E-7	2.99
1/64	1.475E-6	2.03	2.669E-3	1.00	1.360E-8	3.00
1/128	3.638E-7	2.02	1.333E-3	1.00	1.703E-9	3.00

TABLE 5
Errors and convergence rates for Example 5.3 with $\delta = 0.01$

h	$\|u-u_h\|$	rate	$\|u-u\|_{H^1(\Omega)}$	rate	$\|\boldsymbol{p}-\boldsymbol{p}_h\|$	rate
1/128	2.616E-2	1.17	3.801E-0	0.64	2.615E-2	1.17
1/256	9.421E-3	1.47	2.012E-0	0.91	9.421E-3	1.47
1/512	2.515E-3	1.91	8.461E-1	1.25	2.515E-3	1.91
h	$\|\nabla\cdot(\boldsymbol{p}-\boldsymbol{p}_h)\|$	rate	$\|\nabla\cdot(\boldsymbol{\beta}(u-u_h))\|$	rate	$\|z_h\|$	rate
1/128	2.616E-3	1.17	3.435E-1	0.36	1.375E-6	2.25
1/256	9.421E-4	1.47	2.362E-1	0.54	2.367E-7	2.54
1/512	2.515E-4	1.91	1.423E-1	0.73	3.200E-8	2.89

(a) order=1

h	$\|u-u_h\|$	rate	$\|u-u\|_{H^1(\Omega)}$	rate	$\|\boldsymbol{p}-\boldsymbol{p}_h\|$	rate
1/128	4.470E-3	1.77	1.123E-0	1.25	4.470E-3	1.77
1/256	8.402E-4	2.41	3.103E-1	1.86	8.402E-4	2.41
1/512	8.442E-5	3.31	5.018E-2	2.63	8.441E-5	3.32
h	$\|\nabla\cdot(\boldsymbol{p}-\boldsymbol{p}_h)\|$	rate	$\|\nabla\cdot(\boldsymbol{\beta}(u-u_h))\|$	rate	$\|z_h\|$	rate
1/128	4.470E-4	1.77	6.839E-2	1.06	8.267E-8	2.91
1/256	8.402E-5	2.41	2.610E-3	1.39	7.847E-9	3.39
1/512	8.442E-6	3.32	7.817E-3	1.74	5.088E-10	3.94

(b) order =2

To test the robustness of our method for the pure convection problem, in Figure 2 we show the numerical solutions for Example 3 with $k = 1$ and upon $\delta = 0.001$ on structured meshes with various mesh sizes. We observe that, even for the highly sharp internal layer problem on relatively coarse meshes, the numerical solutions show no

sighs of global spurious oscillation. When the mesh size does not resolve the layer only mild and localized oscillation presents around the internal layer.

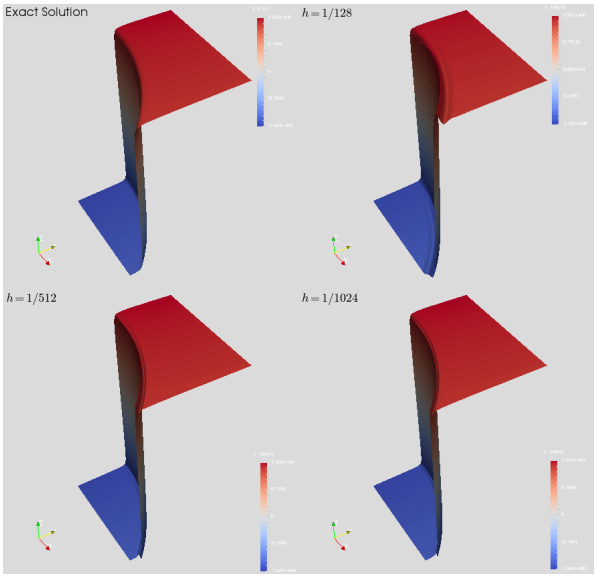


FIG. 2. *Various numerical solutions for Example 5.2 with* $\delta = 0.001$

6. Outflow Boundary Layers. From Figure 1 we see that the current method does not handle outflow boundary well because its lack of upstream mechanism. In this section we propose two simple modifications of the method based on the current setting that removes the global spurious oscillation. More specifically, one method impose the boundary condition weakly, whereas the other takes the approach of weighting the stabilizer such that the oscillation is more "costly" closer to the inflow boundary, and, hence, introduces a notion of upwind direction.

6.1. Weakly imposed boundary conditions. In this approach we weakly impose the Dirichlet boundary conditions, giving different weight to the inflow and outflow boundary. The modified weak formulation is to find $(u_h, \boldsymbol{p}_h, z_h) \in V_h^k \times RT^k \times X_h^k$ such that

$$\mathcal{A}_1[(u_h, \boldsymbol{p}_h, z_h), (v_h, \boldsymbol{q}_h, x_h)] = l_h(x_h), \quad \forall\, (v_h, \boldsymbol{q}_h, x_h) \in V_h^k \times RT^k \times X_h^k, \tag{6.1}$$

where

$$\begin{aligned}\mathcal{A}_1[(u_h, \boldsymbol{p}_h, z_h), (v_h, \boldsymbol{q}_h, x_h)] &= b(\boldsymbol{q}_h, v_h, z_h) + b(\boldsymbol{p}_h, u_h, x_h) + s[(u_h, \boldsymbol{p}_h), (v_h, \boldsymbol{q}_h)] \\ &\quad + \left\langle (h[\beta \cdot \boldsymbol{n}]_-^2 + \gamma \epsilon^2 / h) u, v \right\rangle_{\partial\Omega}\end{aligned}$$

and

$$l_h(x_h) = (f, x_h) + \left\langle (h[\beta \cdot \boldsymbol{n}]_-^2 + \gamma \epsilon^2 / h) g, v \right\rangle_{\partial\Omega}.$$

In the above formulation $[\beta \cdot n]_- = \min(0, \beta \cdot n)$ and $\epsilon = \min(\lambda_A)$, i.e., the smallest eigenvalue of A.

Remark 6.1. Note that in the above method the Dirichlet boundary condition is enforced weakly everywhere. Alternatively one may impose the Dirichlet conditions strongly on the inflow boundary. The outcome turns out to be similar.

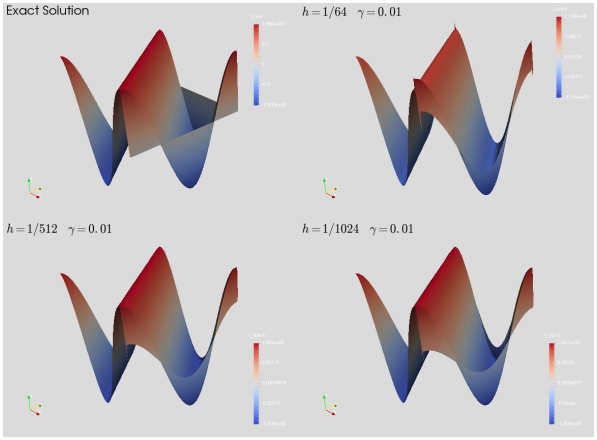


FIG. 3. *Various numerical solutions of Example 5.1 with weakly imposed Dirichlet condition*

Figure 3 shows the numerical solutions for Example 5.1 computed by using the method (6.1) on the same meshes in Figure 1 for $\epsilon = 0.002$. Comparing to Figure 1 the spurious oscillation is completely removed and only a mild local oscillation is observed for the coarsest mesh on the outflow boundary layers.

We also test the method on a commonly used benchmark problem with an internal and outflow boundary layers [7].

EXAMPLE 6.1. *Let u be the solution that satisfies*

$$\begin{aligned} \nabla \cdot (\boldsymbol{\beta} u - \epsilon \nabla u) &= 0 \quad \text{on } \Omega, \\ u &= 1 \quad \text{on } \Gamma_L, \\ u &= 0 \quad \text{on } \partial\Omega \setminus \Gamma_L \end{aligned}$$

where Ω is the unit square domain $(0,1)^2$, $\beta = (1, -0.5)$ and Γ_L is the left boundary of the square, i.e., $x = 0$. ϵ is the diffusion coefficient and in out test we choose $\epsilon = 0.001$ in which case the internal and boundary layers are very sharp.

In Figure 4 we compare the results between the original method (see figures on the top) and the method of (6.1) (see figures at the bottom). We observe that the weak boundary condition method results in an accurate solution in the bulk, with unresolved layers, that are resolved as the mesh-size is small enough, whereas the approximation with strongly imposed conditions has a globally large error.

6.2. Weighted stabilization method. In this subsection we propose a method where a weight function is introduced in the stabilizing term s. The motivation here is to change the stabilization making oscillations more "costly" closer to the inflow boundary, this way introducing a notion of upwind direction. More precisely, we introduce a weight function $\eta : \Omega \to \mathbb{R}$ such that

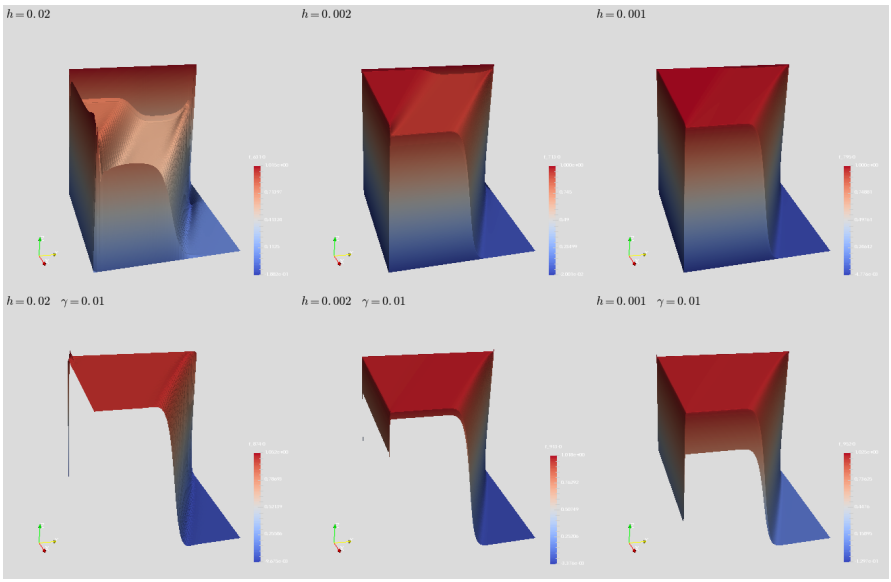
$$\beta > 0 \quad \text{and} \quad \boldsymbol{\beta} \cdot (\nabla \eta) < 0. \tag{6.2}$$

For Example 5.3 we choose

$$\eta = 3 - \boldsymbol{\beta} \cdot (x, y)$$

and for Example 6.1 we choose

$$\eta = 2 - \boldsymbol{\beta} \cdot (x, y).$$



(a) (b) (c)

FIG. 4. *Numerical performance of the weak boundary method for Example 6.1.*

It is easy to check that (6.2) holds for both problems. We then introduce η^p, for some $p > 0$ to be specified, as a weight in s.

The finite element setting is then to find $(u_h, \boldsymbol{p}_h, z_h) \in V_{g,D}^k \times RT^k \times X_h^k$ such that

$$\mathcal{A}_2[(u_h, \boldsymbol{p}_h, z_h), (v_h, \boldsymbol{q}_h, x_h)] = l_h(x_h), \quad \forall\, (v_h, \boldsymbol{q}_h, x_h) \in V^k \times RT^k \times X_h^k, \tag{6.3}$$

where

$$\mathcal{A}_2[(u_h, \boldsymbol{p}_h, z_h), (v_h, \boldsymbol{q}_h, x_h)] = b(\boldsymbol{q}_h, v_h, z_h) + b(\boldsymbol{p}_h, u_h, x_h) + s_\eta[(u_h, \boldsymbol{p}_h), (v_h, \boldsymbol{q}_h)],$$

$$s_\eta[(u_h, \boldsymbol{p}_h), (v_h, \boldsymbol{q}_h)] = (\eta^p(\boldsymbol{p} + A\nabla u - \boldsymbol{\beta} u), (\boldsymbol{q} + A\nabla v - \boldsymbol{\beta} v))$$

and

$$l_h(x_h) = (f, x_h).$$

Figure 5 shows the numerical solutions for Example 5.1 computed by using the method of (6.3) on the same meshes in Figure 1 for $\epsilon = 0.002$. Comparing to Figure 1 we observe that the global spurious oscillation has been eliminated even for very coarse mesh. Local oscillations along the outflow boundary does appear when the layer is not completely resolved. We also test this method for Example 6.1 (see results in Figure 6).

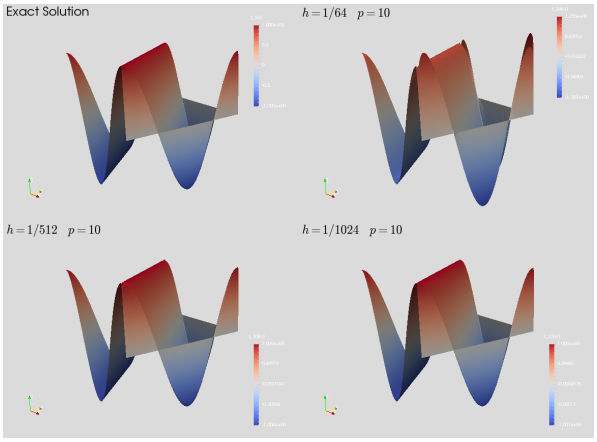
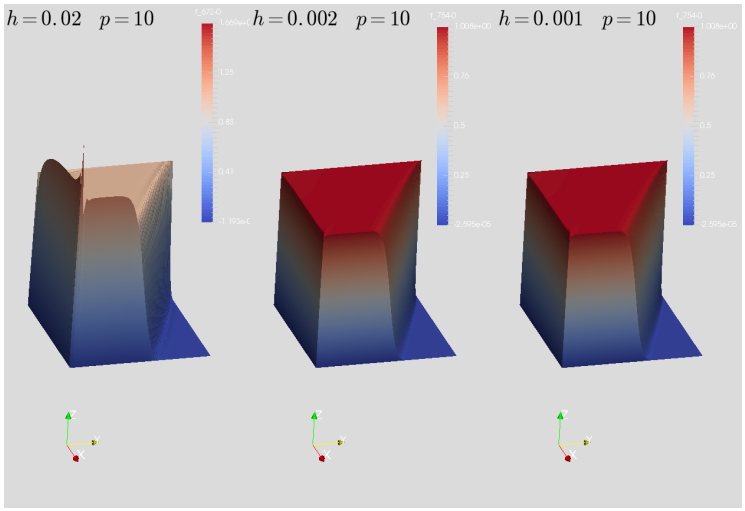


FIG. 5. *Various numerical solutions with weighted stabilization method for Example 5.1*



(a) (b) (c)

FIG. 6. *Numerical performance of the weighted stabilization method.*

REFERENCES

[1] I. Babuška, *Error-bounds for finite element method*, Numerische Mathematik, 16 (1971), pp. 322–333, https://doi.org/10.1007/BF02165003.

[2] C. Bacuta and J. Jacavage, *A nonconforming saddle point least squares approach for elliptic interface problems*, ArXiv e-prints, (2018), https://arxiv.org/abs/1808.10409.

[3] C. Bacuta and K. Qirko, *A saddle point least squares approach for primal mixed formulations of second order PDEs*, Comput. Math. Appl., 73 (2017), pp. 173–186, https://doi.org/10.1016/j.camwa.2016.11.014.

[4] J. H. Bramble, R. D. Lazarov, and J. E. Pasciak, *A least-squares approach based on a discrete minus one inner product for first order systems*, Math. Comp., 66 (1997), pp. 935–955, https://doi.org/10.1090/S0025-5718-97-00848-X.

[5] S. C. Brenner, *Poincare-friedrichs inequalities for piecewise h(1) functions*, SIAM J. Numer. Anal., 41 (2003), pp. 306–324, https://doi.org/10.1137/S0036142902401311.

[6] A. N. Brooks and T. J. R. Hughes, *Streamline upwind/Petrov-Galerkin formulations for convection dominated flows with particular emphasis on the incompressible Navier-Stokes equations*, Comput. Methods Appl. Mech. Engrg., 32 (1982), pp. 199–259, https://doi.org/10.1016/0045-7825(82)90071-8.

[7] E. Burman, *A unified analysis for conforming and nonconforming stabilized finite element methods using interior penalty*, SIAM J. Numer. Anal., 43 (2005), pp. 2012–2033, https://doi.org/10.1137/S0036142903437374.

[8] E. Burman, *Stabilized finite element methods for nonsymmetric, noncoercive, and ill-posed problems. Part I: Elliptic equations*, SIAM J. Sci. Comput., 35 (2013), pp. A2752–A2780, https://doi.org/10.1137/130916862.

[9] E. Burman, *Error estimates for stabilized finite element methods applied to ill-posed problems*, C. R. Math. Acad. Sci. Paris, 352 (2014), pp. 655–659, https://doi.org/10.1016/j.crma.2014.06.008.

[10] E. Burman, *Robust error estimates in weak norms for advection dominated transport problems with rough data*, Mathematical Models and Methods in Applied Sciences, 24 (2014), pp. 2663–2684, https://doi.org/10.1142/S021820251450033X.

[11] E. Burman, *Stabilized finite element methods for nonsymmetric, noncoercive, and ill-posed problems. Part II: Hyperbolic equations*, SIAM J. Sci. Comput., 36 (2014), pp. A1911–A1936, https://doi.org/10.1137/130931667.

[12] E. Burman, *Stabilised finite element methods for ill-posed problems with conditional stability*, Lecture Notes in Computational Science and Engineering, 114 (2016), pp. 93–127, https://doi.org/10.1007/978-3-319-41640-3_4.

[13] E. Burman and P. Hansbo, *Edge stabilization for Galerkin approximations of convection-diffusion-reaction problems*, Comput. Methods Appl. Mech. Engrg., 193 (2004), pp. 1437–1453, https://doi.org/10.1016/j.cma.2003.12.032.

[14] E. Burman, M. G. Larson, and L. Oksanen, *Primal dual mixed finite element methods for the elliptic Cauchy problem*, ArXiv e-prints, (2017), https://arxiv.org/abs/1712.10172.

[15] E. Burman, L. Oksanen, and M. Nechita, *A stabilized finite element method for inverse problems subject to the convection–diffusion equation. i: diffusion dominated regime.* in preparation.

[16] E. Burman, A. Quarteroni, and B. Stamm, *Interior penalty continuous and discontinuous finite element approximations of hyperbolic equations*, J. Sci. Comput., 43 (2010), pp. 293–312, https://doi.org/10.1007/s10915-008-9232-6.

[17] I. Capuzzo-Dolcetta and S. Finzi Vita, *Finite element approximation of some indefinite elliptic problems*, Calcolo, 25 (1988), pp. 379–395 (1989), https://doi.org/10.1007/BF02575842, https://doi.org/10.1007/BF02575842.

[18] C. Chainais-Hillairet and J. Droniou, *Finite-volume schemes for noncoercive elliptic problems with Neumann boundary conditions*, IMA J. Numer. Anal., 31 (2011), pp. 61–85, https://doi.org/10.1093/imanum/drp009, https://doi.org/10.1093/imanum/drp009.

[19] J. Chan, J. A. Evans, and W. Qiu, *A dual Petrov-Galerkin finite element method for the convection-diffusion equation*, Comput. Math. Appl., 68 (2014), pp. 1513–1529, https://doi.org/10.1016/j.camwa.2014.07.008.

[20] P. Ciarlet, Jr., *T-coercivity: application to the discretization of Helmholtz-like problems*, Comput. Math. Appl., 64 (2012), pp. 22–34, https://doi.org/10.1016/j.camwa.2012.02.034.

[21] P. G. Ciarlet, *The finite element method for elliptic problems*, North-Holland Publishing Co., Amsterdam-New York-Oxford, 1978. Studies in Mathematics and its Applications, Vol. 4.

[22] B. Cockburn and C.-W. Shu, *TVB Runge-Kutta local projection discontinuous Galerkin finite element method for conservation laws. II. General framework*, Math. Comp., 52 (1989),

pp. 411–435, https://doi.org/10.2307/2008474.

[23] R. Codina, *Stabilization of incompressibility and convection through orthogonal sub-scales in finite element methods*, Comput. Methods Appl. Mech. Engrg., 190 (2000), pp. 1579–1599, https://doi.org/10.1016/S0045-7825(00)00254-1.

[24] H. B. Da Veiga, *On a stationary transport equation*, Annali dell'Università di Ferrara, 32 (1986), pp. 79–91, https://doi.org/10.1007/BF02825238.

[25] W. Dahmen, C. Huang, C. Schwab, and G. Welper, *Adaptive Petrov-Galerkin methods for first order transport equations*, SIAM J. Numer. Anal., 50 (2012), pp. 2420–2445, https://doi.org/10.1137/110823158.

[26] L. Demkowicz and J. Gopalakrishnan, *A class of discontinuous Petrov-Galerkin methods. Part I: the transport equation*, Comput. Methods Appl. Mech. Engrg., 199 (2010), pp. 1558–1572, https://doi.org/10.1016/j.cma.2010.01.003.

[27] J. Douglas, Jr. and T. Dupont, *Interior penalty procedures for elliptic and parabolic Galerkin methods*, in Computing methods in applied sciences, (1976), pp. 207–216, https://doi.org/10.1007/BFb0120591.

[28] A. Ern and J.-L. Guermond, *Theory and practice of finite elements*, vol. 159 of Applied Mathematical Sciences, Springer-Verlag, New York, 2004, https://doi.org/10.1007/978-1-4757-4355-5.

[29] A. Ern and J.-L. Guermond, *Finite element quasi-interpolation and best approximation*, ESAIM-Math. Model. Numer. Anal.-Model. Math. Anal. Numer., 51 (2017), pp. 1367–1385, https://doi.org/10.1051/m2an/2016066.

[30] J.-L. Guermond, *Stabilization of Galerkin approximations of transport equations by subgrid modeling*, M2AN Math. Model. Numer. Anal., 33 (1999), pp. 1293–1316, https://doi.org/10.1051/m2an:1999145.

[31] T. J. R. Hughes, G. Engel, L. Mazzei, and M. G. Larson, *The continuous Galerkin method is locally conservative*, J. Comput. Phys., 163 (2000), pp. 467–488, https://doi.org/10.1006/jcph.2000.6577.

[32] C. Johnson, U. Nävert, and J. Pitkäranta, *Finite element methods for linear hyperbolic problems*, Comput. Methods Appl. Mech. Engrg., 45 (1984), pp. 285–312, https://doi.org/10.1016/0045-7825(84)90158-0.

[33] C. Johnson and J. Pitkäranta, *An analysis of the discontinuous Galerkin method for a scalar hyperbolic equation*, Math. Comp., 46 (1986), pp. 1–26, https://doi.org/10.2307/2008211.

[34] K. Kavaliou and L. Tobiska, *A finite element method for a noncoercive elliptic problem with Neumann boundary conditions*, Comput. Methods Appl. Math., 12 (2012), pp. 168–183, https://doi.org/10.2478/cmam-2012-0011, https://doi.org/10.2478/cmam-2012-0011.

[35] Y. Liu, J. Wang, and Q. Zou, *A Conservative Flux Optimization Finite Element Method for Convection-Diffusion Equations*, ArXiv e-prints, (2017), https://arxiv.org/abs/1710.08082.

[36] A. Logg, K.-A. Mardal, and G. Wells, *Automated solution of differential equations by the finite element method: The FEniCS book*, vol. 84, Springer Science & Business Media, 2012, https://doi.org/10.1007/978-3-642-23099-8.

[37] W. F. Mitchell, *A collection of 2d elliptic problems for testing adaptive grid refinement algorithms*, Applied mathematics and computation, 220 (2013), pp. 350–364, https://doi.org/10.1016/j.amc.2013.05.068.

[38] P. Monk and E. Süli, *The adaptive computation of far-field patterns by a posteriori error estimation of linear functionals*, SIAM J. Numer. Anal., 36 (1999), pp. 251–274, https://doi.org/10.1137/S0036142997315172.

[39] C. Wang and J. Wang, *A Primal-Dual Weak Galerkin Finite Element Method for Fokker-Planck Type Equations*, ArXiv e-prints, (2017), https://arxiv.org/abs/1704.05606.

[40] C. Wang and J. Wang, *A primal-dual weak Galerkin finite element method for second order elliptic equations in non-divergence form*, Math. Comp., 87 (2018), pp. 515–545, https://doi.org/10.1090/mcom/3220.

[41] C. Wang and J. Wang, *Primal-Dual Weak Galerkin Finite Element Methods for Elliptic Cauchy Problems*, ArXiv e-prints, (2018), https://arxiv.org/abs/1806.01583.